EUROPEAN JOURNAL OF PURE AND APPLIED MATHEMATICS
2026, Vol. 19, Issue 2, Article Number 7076
ISSN 1307-5543 – ejpam.com
Published by New York Business Global

Nonlinear Variable-Order Fractional System with Application to Chaotic Dynamics and Adaptive Fixed-Time Fractional-Order Sliding Mode Control

Saim Ahmed[1,*], Hasib Khan[3,4], Jehad Alzabut[3,5], Ahmad Taher Azar[1,2], Rajermani Thinakaran[6]

[1] *Automated Systems and Computing Lab (ASCL), Prince Sultan University, 11586 Riyadh, Saudi Arabia*
[2] *College of Computer and Information Sciences, Prince Sultan University, Riyadh, Saudi Arabia*
[3] *Department of Mathematics and Sciences, Prince Sultan University, 11586 Riyadh, Saudi Arabia*
[4] *Department of Mathematics, Shaheed Benazir Bhutto University, Sheringal PO Box 18000, Dir Upper, Khyber Pakhtunkhwa, Pakistan*
[5] *Department of Industrial Engineering, OSTIM Technical University, 06374, Ankara, Turkey*
[6] *Faculty of Data Science and Information Technology, INTI International University, Malaysia*

Abstract. In this paper, a theoretical and computational analysis is established for a new general class of variable order (VO) system of fractional differential equations (FDEs). The theoretical findings are based on the literature on the fixed point theorems (FPTs) and stability of Hyers-Ulam (HU). Banach's fixed point theorem (FPT) is used to check the uniqueness of the solutions of the presumed system. Leray-Schauder's (LS) approach is utilized to study solution existence. A computational iterative numerical technique is developed. In addition, a control approach is devised for the fractional-order dynamical power system, employing adaptive fixed-time fractional-order sliding mode control. The main objective is to effectively control the chaotic power system. Therefore, a fractional-order sliding mode control method is devised with the objective of achieving superior tracking performance and ensuring smooth control inputs. Subsequently, an adaptive method is employed to mitigate the effects of the unknown disturbance. The Lyapunov theorem is employed to investigate the overall dynamical system. The comparative results are demonstrated to give a deeper understanding of the study and show that the suggested approach has better tracking control and convergence capabilities as process innovation.

2020 Mathematics Subject Classifications: 62F35, 93C15, 93D20

*Corresponding Author.
DOI: https://doi.org/10.29020/nybg.ejpam.v19i2.7076

Email addresses: `sahmed@psu.edu.sa` (Saim Ahmed)
`hkhan@psu.edu.sa` (H. Khan),
`jalzabut@psu.edu.sa, jehad.alzabut@ostimteknik.edu.tr` (J. Alzabut)
`aazar@psu.edu.sa, ahmad_t_azar@ieee.org` (A.T. Azar),
`rajermani.thina@newinti.edu.my` (R. Thinakaran)

Key Words and Phrases: Riemann-Liouville derivative, positive solutions, power system, adaptive fractional sliding mode control, fixed-time stability.

1. Introduction

Fractional calculus (FC) is a mathematical framework that expands the concepts of integration and differentiation to encompass non-integer orders [1–4]. A diverse group of scientists, comprising physicists, engineers, mathematicians, and other experts, currently take part in the investigation and evaluation of this nascent field of study. Leibniz, Euler, and Laplace made significant contributions to the establishment of the discipline of fluid dynamics during the 18th century. In recent years, there has been a notable rise in interest surrounding a wide range of applications within the domains of physics, engineering, finance, and signal processing. The fractional calculus (FC) is a mathematical framework that pertains to the differentiation and integration of non-integer orders. This stands in contrast with standard calculus, which is confined to operations involving only integer orders. The concept of FC is also regarded as significant in the examination of various scientific and engineering disciplines. [5–8]. Furthermore, this approach exhibits usefulness in the examination of financial assets, namely in the assessment of stock values. Additionally, it finds relevance in the analysis of fractal patterns and long-term memory signals within the realm of data processing. The application of FC has been discovered to enhance the preservation of long-term memory and enable the analysis of fractal patterns of behavior. The classical calculus exhibits limitations in its ability to effectively preserve information and handle events as distinct entities, hence making it unsuitable for such systems. The use of FC offers an improved structure for modeling processes by considering the attributes of long-term memory and the fractal nature of systems. Extensive scientific and technical research efforts have been devoted to the mathematical modeling and numerical simulation of dynamical systems. The developmental path of fractional order operators encompasses a diverse array of kernels, encompassing both local and non-local variations, as well as singular and non-singular manifestations. Several scholars have been discovered in recent studies regarding these issues. Academic researchers are afforded the opportunity to have access to and critically evaluate a noteworthy literary work [9, 10].

Variable-order fractional differential equations (VFDs) are a significant advancement in the field of fractional calculus because they provide a flexible structure for describing complex dynamic systems with non-local memory effects [11]. These broadened the application of traditional calculus by including fractional-order derivatives that change with time, space, or other variables [12, 13]. VFDs are used in a variety of scientific domains because they can capture complex behaviors that standard models lack. The inclusion of fractional derivatives of various orders that can react to dynamic system changes defines VFDs [14–16]. VFDs offer a more realistic representation of complex systems than ODEs, as the sequence of differentiation in them is flexible. The ability to account for variations in the order of derivatives is necessary for modeling time-dependent processes incorporating memory effects, such as those present in viscoelastic materials, anomalous diffusion, and biological systems. In mathematical terms, a VDE can be expressed in the form $D^{\alpha(t)}u(t) = f(u)$ where $\alpha(t)$ varies with respect to t. The variability of VFDs for $\alpha(t)$ can be estimated using behavior, environmental factors, and control inputs. This adaptability has proven useful in modeling phenomena like transient behaviors in materials or biological processes that are stimulated by the environment, enabling a more accurate representation of these phenomena [17, 18].

MOdeling and simulations and AI applications are common these days in almost all walks of life. One can see the results in [19–23]. Solving VFDs analytically is particularly difficult due to the non-locality of fractional derivatives and the changeable order. Approximate solutions to VFDs can be found by the use of a number of different computational methods, such as fractional differences, Grünwald-Letnikov schemes, and fractional Adams-Bashforth approaches. The variable order fractional differential equations are a useful mathematical tool for modeling time-varying or externally induced changes in dynamic systems with memory effects. Because of their applicability across a wide range of scientific disciplines, they are an invaluable resource for modern scientists. The theory and numerical approaches related to VFDs are still being studied and improved, opening the door to more accurate modeling and a deeper understanding of real-world processes.The power system, which is considered a prominent example of a nonlinear dynamical system, has been seen to exhibit nonlinear dynamic properties. As a result, there has been a significant amount of research conducted on the chaotic oscillations that arise from these characteristics [24]. The reliable operation of power systems can be significantly affected by the emergence of chaotic oscillation. This can result in various possible consequences, like voltage collapse, angle instability, and even the development of large-scale blackout episodes within the system [25]. Furthermore, it is important to acknowledge that a power system that is interrelated exhibits some key characteristics, including its multivariable nature, nonlinearity, and strong coupling dynamics [26]. The presence of these intrinsic qualities possesses the capacity to generate temporary volatility within the power system. Therefore, the management of the turbulent oscillations within the power system is crucial in ensuring the stability of its dynamics.

Numerous control strategies have been proposed in the literature to mitigate the oscillations in chaotic power systems. These strategies include a synchronization characteristics scheme using a continuous feedback control method [27], linear state feedback control method [28], adaptive backstepping control approach [29], adaptive terminal sliding mode [30], and adaptive synergetic scheme [31]. These control strategies that have been provided exhibit effectiveness in exploring the reduction of chaotic oscillations within power systems. Nevertheless, these methodologies solely attain the asymptotic convergence of state variables without the ability to ensure their precise convergence within a given time frame. In literature, the majority of authors primarily focus on analyzing 2nd-order power systems, with limited consideration given to the control of more intricate power system models. The 2nd-order system is derived from the 4th-order power system, and extensive research has been conducted on the chaotic behavior shown by the four-order power system [32–36]. Hence, it is imperative to have direct control over the four-order power system.

Nonlinear sliding surfaces are utilized by the terminal sliding mode controller to ensure that errors converge to the origin in finite time, and that accuracy increases as the sliding surface is attained. The nonlinear structure of the terminal sliding mode control (TSMC) provides a faster convergence rate compared to conventional SMC [37]. Noise attenuation, parametric uncertainty compensation, and finite-time convergence are its advantages. TSMC has been used to control the dynamics of chaotic power systems. A method has been shown to solve the finite-time boundedness (FTB) problem for a nonlinear description photovoltaic (PV) system using the finite-time fuzzy SMC scheme [38]. In [36], the authors have presented an approach for mitigating chaotic oscillations in a power system with a fourth-order chaos model, through the implementation of an SMC based on exponential reaching law. Since finite time is dependent on the initial values, thus, fixed time can be utilized to design a control scheme independent on the initial values [39]. Therefore, the fixed time integral SMC has been proposed for the suppression of oscillation in chaotic power systems [33]. An approach has been presented to stabilize nonlinear power systems using a fixed-time fractional-order SMC [35]. This controller demonstrates successful stabilization of a nonlinear power system, as evidenced by the nonlinear behavior observed in the state trajectories of the power system. Adaptive control excels at adjusting to unknown dynamics and improving closed-loop monitoring. If the parameters/dynamics are unknown, an adaptive scheme can be used to estimate them. Thus, the literature has suggested a number of different approaches for SMC-based adaptive systems [40, 41].

For a better description of the paper, we have divided the paper in several partitions that highlight the mathematical and computational works related to a system of nonlocal VO integro-differential equations. The division of the paper is made on the aspects of qualitative analysis, numerical algorithms and computations, and fractional order optimization.

- The qualitative analysis is divided into further three sections:

i The existence of a solution for the VO system of FDEs.

ii The uniqueness criteria for the VO-ID-system.

iii Hyers-Ulam stability. The numerical section is further divided into two subsections including a) the computational scheme for the VO-ID-system b) a comparative study of the numerical results for different variable orders

- An adaptive fixed-time fractional-order sliding mode control scheme has been proposed with the objective of obtaining good tracking, chatter-free control input, and error convergence in fixed time
- The utilization of adaptive control combined with fractional SMC has been employed as a means to counterbalance the effects of unknown dynamics.
- Furthermore, an examination of the fixed-time stability of the nonlinear power system is conducted by Lyapunov analysis.

The subsequent sections are categorized in the following manner: the second section provides a comprehensive analysis of the relevant literature. The preliminary information is provided in Section 2. In Section 3 of the paper, we focused on the examination of the VO system of FDEs. Section 4 presents the establishment of HUS. The iterative scheme employed by the application is described in Section 5. The developed control method and the stability analyses using the Lyapunov criterion are presented in Section 6. The numerical results of the closed-loop model using the proposed scheme are given in Section 7. Section 8 presents the discussion on the obtained results. Section 9 concludes this work.

2. Preliminaries

The history of FDEs is lengthy and dynamic, behaviour, physical circumstances, and control inputs can all be used to estimate the variability of fractional operators in many areas of science and technology. Due to their capacity to explain phenomena including memory and long-range dependence, higher-order DEs are a strong tool for modelling systems that contradict conventional integer-order descriptions. The applications of FDEs are expected to grow more as the field develops [9, 10].

Here, we highlight some notions from the literature regarding the RL calculus that will be considered to obtain the main works of the paper.

Definition 1. *[9] Fractional order RL integral and derivative for non-variable orders of $g(x)$ are given below*

$$ {}_a\mathbb{I}_x^{\vartheta^*} g(x) = \frac{1}{\Gamma(\vartheta^*)} \int_a^x \frac{g(\tau)}{(x-\tau)^{1-\vartheta^*}} d\tau, \tag{1} $$

$$ {}_a\mathbb{D}_x^{\vartheta^*} g(x) = \frac{1}{\Gamma(1-\vartheta^*)} \frac{d}{dt} \int_a^x \frac{g(\tau)}{(x-\tau)^{\vartheta^*}} d\tau, \tag{2} $$

for $b-1 < \vartheta^* < b$, $b \in \aleph$ and $\Gamma(\vartheta^*)$ is

$$ \Gamma(\vartheta^*) = \int_0^\infty e^{-x} x^{\vartheta^*-1} dt. $$

The following VO operators are taken from [42].

Definition 2. *The VO time FI is given below*

$$ {}_a\mathbb{I}_x^{\vartheta^*(x)} g(x) = \frac{1}{\Gamma(\vartheta^*(x))} \int_a^x (x-s)^{\vartheta^*(x)-1} g(s) ds, \tag{3} $$

where $n-1 < \vartheta^*(x) < n$, is a variable order.

Definition 3. *The left side VO time FD in RL-sense is given below*

$$ {}_a\mathbb{D}_x^{\vartheta^*(x)} g(x) = \frac{1}{\Gamma(n-\vartheta^*(x))} \frac{d^n}{dx^n} \int_a^x (x-s)^{n-\vartheta^*(t)-1} g(s) ds, \tag{4} $$

where $n-1 < \vartheta^*(x) < n$, is a variable order.

Definition 4. *The right side VO time FD in RL-sense is given below*

$$ {}_a\mathbb{D}_x^{\alpha(x)} g(x) = \frac{(-1)^n}{\Gamma(n-\alpha(x))} \frac{d^n}{dt^n} \int_a^x (x-s)^{n-\alpha(t)-1} g(s) ds, \tag{5} $$

where $n-1<\alpha(x)<n$, is a variable order.

Lemma 1. *[41] For the stability of fixed-time convergence for the system $\dot{y}(x) = f(x,y),\ \ y(0) = y_0$, the Lyapunov function $V(y)$ that satisfies*
i. $V(y) = 0 \ \Leftrightarrow \ y = 0$
ii. $\dot{V}(y) \leq -w_1 V(y)^{v_1} - w_2 V(y)^{v_2}$
for $w_1, w_2 > 0$, $0 < v_1 < 1$ and $v_2 > 1$. So, the fixed-time T is obtained as

$$ T \leq \frac{1}{w_1(1-v_1)} + \frac{1}{w_2(v_2-1)} \tag{6} $$

Lemma 2. *[40] For $\mu_1, \mu_2, ..., \mu_n > 0$, the inequalities satisfy as*

$$ \begin{aligned} &\sum_{i=1}^{n} |\mu_i|^{1+\lambda} \geq \left(\sum_{i=1}^{n} |\mu_i|^2\right)^{\frac{1+\lambda}{2}}, \ for\, 0<\lambda<1 \\ &\sum_{i=1}^{n} |\mu_i|^{\lambda} \geq n^{1-\lambda}\left(\sum_{i=1}^{n} |\mu_i|\right)^{\lambda}, \ for\ \lambda>1 \end{aligned} \tag{7} $$

Property 2.7. [9] The RL derivative satisfies that:

$$ {}_a\mathbb{D}_x^{1-\alpha}\left({}_a\mathbb{D}_x^{\alpha} f(x)\right) = \dot{f}(x), \tag{8} $$
$$ {}_a\mathbb{D}_x^{\alpha}\left({}_a\mathbb{D}_x^{-\alpha} f(x)\right) = f(x) \tag{9} $$

3. The dynamical system

Integro-differential equations, which are a type of mathematical equations that incorporate both differential and integral aspects, have a wide range of applications in several domains. In the field of physics, mathematical models are employed to represent various processes, including but not limited to heat conduction, population dynamics, and electromagnetic wave propagation. Integro-differential equations are utilized in the field of biology to model several biological phenomena, including brain networks, enzyme kinetics, and the spread of epidemics. The utilization of these equations holds significant importance in the field of economics as they facilitate the analysis of investment strategies and the determination of price formation in financial markets. In addition, integro-differential equations find application in the field of engineering for the purpose of forecasting the dynamics of intricate systems, including but not limited to fluid flow in porous media, structural dynamics, and control systems. The inherent adaptability of these tools renders them highly effective in addressing complex challenges across several fields. In this study, we provide a research problem that involves a coupled system of integro-differential equations of VO, specifically focusing on the variable sense of RL derivatives.

$$\begin{aligned}&{}^{R}\mathbb{D}^{\vartheta_i^*(x)}\mathbb{Y}_i(x) = \mathcal{H}_i(x, \frac{1}{\Gamma(\alpha)}\int_0^x (x-s)^{\alpha-1}\mathbb{Y}_i(s)ds),\ x \in \mathrm{I} = [0, T],\\ &\mathbb{Y}_i(x)|_{x=l} = \mathcal{P}_i(x, \mathbb{Y}_i(x)).\end{aligned} \tag{10}$$

The variable order is a $\vartheta_i^*(x) : \mathbb{R} \to (0, 1]$, is the variable order for the Riemann-Liouville derivative ${}^{R}\mathbb{D}^{\vartheta_i^*(x)}$, $\zeta_i \in \mathbb{R}$, the functions $\mathbb{Y}_i : \mathrm{I} \to \mathbb{R}$, $\mathcal{H}_i$, $\mathcal{P}_i$, are continuous functions, for all, $i = 1, 2, \ldots, n$, and satisfying the Caratheodory conditions. The authors' research in the field has revealed that the problem of a system of VO-ID-system with BCs has not yet been explored in terms of solution existence, stability analysis, or computational effort. Various applied dynamical systems can be considered as specific instances of the postulated variable-order system of FDEs. Therefore, looking at the importance of the work, we are considering VO-ID-system (10) for the theoretical findings and computational works based on FPT and numerical scheme, respectively.

Lemma 3. *The following coupled system of VO-ID-system with BCs*

$$\begin{aligned}&{}^{R}\mathbb{D}^{\vartheta_i^*(x)}\mathbb{Y}_i(x)) = \mathcal{H}_i^*(x, \mathcal{I}^{\alpha}\mathbb{Y}_i(x)),\ t \in \mathrm{I} = [0, T],\\ &\mathbb{Y}_i(x)|_{x=l} = \mathcal{P}_i(x, \mathbb{Y}_i(x)),\end{aligned} \tag{11}$$

is equivalent to

$$\begin{aligned}\mathbb{Y}_i(x) = {}& \frac{1}{\Gamma(\vartheta_i^*(x))}\int_0^x (x-s)^{\vartheta_i^*(x)-1}\mathcal{H}_i(s, \frac{1}{\Gamma(\alpha)}\int_0^s (s-r)^{\alpha-1}\mathbb{Y}_i(r)dr)ds + \frac{x^{1-\vartheta_i^*(x)}}{\ell^{1-\vartheta_i^*(x)}}\Big(\mathcal{P}_i(x, \mathbb{Y}_i(x))\\ &- \frac{1}{\Gamma(\vartheta_i^*(x))}\int_0^l (l-s)^{\vartheta_i^*(x)-1}\mathcal{H}_i(s, \frac{1}{\Gamma(\alpha)}\int_0^s (s-r)^{\alpha-1}\mathbb{Y}_i(r)dr)ds\Big),\end{aligned}$$

for $i = 1, 2, \ldots, n$.

Proof. From (19), we have

$${}^{R}\mathbb{D}^{\vartheta_i^*(x)}\mathbb{Y}_i(x)) = \mathcal{H}_i^*(x, \mathcal{I}^{\alpha}\mathbb{Y}_i(x)),\ x \in \mathrm{I} = [0, 1], \qquad \mathbb{Y}_i(x)|_{x=l} = \mathcal{P}_i(x, \mathbb{Y}_i(x)). \tag{12}$$

Applying the VOI of order $\vartheta_i^*(x)$, we have

$$\mathbb{Y}_i(x) = \frac{1}{\Gamma(\vartheta_i^*(x))}\int_0^x (x-s)^{\vartheta_i^*(x)-1}\mathcal{H}_i^*(s, \mathcal{I}^{\alpha}\mathbb{Y}_i(s))ds + C_i x^{1-\vartheta_i^*(x)}. \tag{13}$$

Using the boundary condition $\mathbb{Y}_i(x)|_{x=l} = \mathcal{P}_i(x, \mathbb{Y}_i(x))$, in (13), we have the following equivalent VOI form

$$\mathbb{Y}_i(x) = \frac{1}{\Gamma(\vartheta_i^*(x))}\int_0^x (x-s)^{\vartheta_i^*(x)-1}\mathcal{H}_i(s, \mathcal{I}^{\alpha}\mathbb{Y}_i(s))ds + \frac{x^{1-\vartheta_i^*(x)}}{\ell^{1-\vartheta_i^*(x)}}\Big(\mathcal{P}_i(x, \mathbb{Y}_i(x))$$

$$- \frac{1}{\Gamma(\vartheta_i^*(x))} \int_0^l (l-s)^{\vartheta_i^*(x)-1} \mathcal{H}_i(s, \mathcal{I}^\alpha \mathbb{Y}_i(s)) ds\Big) \tag{14}$$
$$= \frac{1}{\Gamma(\vartheta_i^*(x))} \int_0^x (x-s)^{\vartheta_i^*(x)-1} \mathcal{H}_i(s, \frac{1}{\Gamma(\alpha)} \int_0^s (s-r)^{\alpha-1} \mathbb{Y}_i(r) dr) ds + \frac{x^{1-\vartheta_i^*(x)}}{\ell^{1-\vartheta_i^*(x)}} \Big(\mathcal{P}_i(x, \mathbb{Y}_i(x))$$
$$- \frac{1}{\Gamma(\vartheta_i^*(x))} \int_0^l (l-s)^{\vartheta_i^*(x)-1} \mathcal{H}_i(s, \frac{1}{\Gamma(\alpha)} \int_0^s (s-r)^{\alpha-1} \mathbb{Y}_i(r) dr) ds\Big),$$

where $i = 1, 2, \ldots, n$.

Assume a Banach's space of continuous functions $\mathbb{B} = \{\mathbb{Y}_i(t) : \mathbb{Y}_i(t) \in \mathbb{C}([0,1], \mathbb{R}) \text{ for } t \in [0,1]\}$, having the norm $\|\mathbb{Y}_i\| = \max_{t\in[0,1]} |\mathbb{Y}_i(t)|$. Let $\mathbb{T}_i : \mathbb{C}([0,1], \mathbb{R}) \to \mathbb{C}([0,1], \mathbb{R})$, operators, where

$$\begin{aligned} \mathbb{T}_i \mathbb{Y}_i(x) &= \frac{1}{\Gamma(\vartheta_i^*(x))} \int_0^x (x-s)^{\vartheta_i^*(x)-1} \mathcal{H}_i(s, \frac{1}{\Gamma(\alpha)} \int_0^s (s-r)^{\alpha-1} \mathbb{Y}_i(r) dr) ds + \frac{x^{1-\vartheta_i^*(x)}}{\ell^{1-\vartheta_i^*(x)}} \Big(\mathcal{P}_i(x, \mathbb{Y}_i(x)) \\ &- \frac{1}{\Gamma(\vartheta_i^*(x))} \int_0^l (l-s)^{\vartheta_i^*(x)-1} \mathcal{H}_i(s, \frac{1}{\Gamma(\alpha)} \int_0^s (s-r)^{\alpha-1} \mathbb{Y}_i(r) dr) ds\Big). \end{aligned} \tag{15}$$

By (15), the solutions of the VO-ID-system (10) are the FPs of $\mathbb{T}_i$. The following assumptions is considered:

- (H_1) For some $\zeta_i^1, \zeta_i^2 \in \mathbb{R}_e$, and $\mathbb{U}_i$, $\bar{\mathbb{Y}}_i \in \mathbb{C}$, $t \in [0,k]$, the $\mathcal{H}_i^*$ and $\mathcal{P}_i$, for $i = 1, 2, \ldots, n$ satisfy that

$$|\mathcal{H}_i^*(t, \mathbb{U}_i) - \mathcal{H}_i^*(t, \bar{\mathbb{Y}}_i)| \leq \zeta_i^1 |\mathbb{U}_i - \bar{\mathbb{Y}}_i|,$$
$$|\mathcal{P}_i(t, \mathbb{U}_i) - \mathcal{P}_i(t, \bar{\mathbb{Y}}_i)| \leq \zeta_i^2 |\mathbb{U}_i - \bar{\mathbb{Y}}_i|.$$

Theorem 1. *If for all $i = 1, 2, \ldots, n$, (H_1) is satisfied and we have*

$$\mathcal{H}_i = \max_{x\in[0,T]} \Big\{ \frac{T^{\vartheta_i^*(x)}}{\Gamma(\vartheta_i^*(x)+1)} \frac{\zeta_i^1 T^\alpha}{\Gamma(\alpha+1)} + \frac{x^{1-\vartheta^*(x)}}{l^{1-\vartheta_i^*(x)}} \Big(\zeta_2^i - \frac{l^{\vartheta_i^*(x)}}{\Gamma(\vartheta_i^*(x+1))} \frac{\zeta_i^1 T^\alpha}{\Gamma(\alpha+1)}\Big) \Big\}, \tag{16}$$

with $\mathcal{H}_i < 1$, for $x \in [0,T]$, then the uniqueness of solution for (10) is ensured.

Proof. In this proof, we assume $i = 1, 2, \ldots, n$. Let us consider that: $\sup_{x\in[0,T]} |\mathcal{H}_i^*(x,0)| = \wp_1 < \infty$, and $\sup_{t\in[0,k]} |\mathcal{P}_i(x,0)| = \wp_2 < \infty$, $\mathbb{S}_{\eta_i} = \{\mathbb{Y}_i \in \mathbb{C}([0,k], \mathbb{R}_e) : \|\mathbb{Y}_i\| < \eta_i\}$, and $k \geq 1$. For $\mathbb{Y}_i \in \mathbb{S}_{\eta_i}$, and $x \in [0,T]$, then using (H_1), we proceeded to

$$\begin{aligned} |\mathcal{H}_i(x, \frac{1}{\Gamma(\alpha)} \int_0^x (x-r)^{\alpha-1} \mathbb{Y}_i(r) dr)| &= \big|\mathcal{H}_i(x, \frac{1}{\Gamma(\alpha)} \int_0^x (x-r)^{\alpha-1} \mathbb{Y}_i(r) dr) - \mathcal{H}_i(x,0) + \mathcal{H}_i(x,0)\big| \\ &\leq |\mathcal{H}_i(x, \frac{1}{\Gamma(\alpha)} \int_0^x (x-r)^{\alpha-1} \mathbb{Y}_i(r) dr) - \mathcal{H}_i(x,0)| + |\mathcal{H}_i(x,0)| \\ &\leq \frac{\zeta_i^1 T^\alpha}{\Gamma(\alpha+1)} \|\mathbb{Y}_i(x)\| + |\mathcal{H}_i(x,0)| \end{aligned} \tag{17}$$

$$\leq \frac{\eta_i \zeta_i^1 T^\alpha}{\Gamma(\alpha+1)} + \wp_1.$$

Also, for $\mathbb{Y}_i \in \mathbb{S}_{\eta_i}$, $t \in [0,k]$, one has

$$\begin{aligned} |\mathcal{P}_i(x,\mathbb{Y}_i(x))| &= |\mathcal{P}_i(x,\mathbb{Y}_i(x)) - \mathcal{P}_i(x,0) + \mathcal{P}_i(x,0)| \\ &\leq |\mathcal{P}_i(x,\mathbb{Y}_i(x)) - \mathcal{P}_i(x,0)| + |\mathcal{P}_i(x,0)| \\ &\leq \zeta_i^2 \|\mathbb{Y}_i(x)\| + |\mathcal{P}_i(x,0)| \\ &\leq \zeta_i^2 \eta_i + \wp_2. \end{aligned} \tag{18}$$

With the help of (15), (17) and (18), the following boundedness is ensured

$$\begin{aligned} |\mathbb{T}_i\mathbb{Y}_i(x)| = &\Big|\frac{1}{\Gamma(\vartheta_i^*(x))}\int_0^x (x-s)^{\vartheta_i^*(x)-1}\mathcal{H}_i(s, \frac{1}{\Gamma(\alpha)}\int_0^s (s-r)^{\alpha-1}\mathbb{Y}_i(r)dr)ds + \frac{x^{1-\vartheta_i^*(x)}}{\ell^{1-\vartheta_i^*(x)}}\Big(\mathcal{P}_i(x,\mathbb{Y}_i(x)) \\ &- \frac{1}{\Gamma(\vartheta_i^*(x))}\int_0^l (l-s)^{\vartheta_i^*(x)-1}\mathcal{H}_i(s, \frac{1}{\Gamma(\alpha)}\int_0^s (s-r)^{\alpha-1}\mathbb{Y}_i(r)dr)ds\Big)\Big| \\ &\leq \Big|\frac{1}{\Gamma(\vartheta_i^*(x))}\int_0^x (x-s)^{\vartheta_i^*(x)-1}(\frac{\eta_i\zeta_i^1 T^\alpha}{\Gamma(\alpha+1)} + \wp_1))ds + \frac{x^{1-\vartheta_i^*(x)}}{\ell^{1-\vartheta_i^*(x)}}\Big(\zeta_i^2\eta_i + \wp_2 \\ &- \frac{1}{\Gamma(\vartheta_i^*(x))}\int_0^l (l-s)^{\vartheta_i^*(x)-1}(\frac{\eta_i\zeta_i^1 T^\alpha}{\Gamma(\alpha+1)} + \wp_1))ds\Big) \\ &\leq \max_{x\in[0,T]}\Big\{\frac{1}{\Gamma(\vartheta_i^*(x)+1)}T^{\vartheta_i^*(x)}(\frac{\eta_i\zeta_i^1 T^\alpha}{\Gamma(\alpha+1)} + \wp_1)) + \frac{x^{1-\vartheta_i^*(x)}}{\ell^{1-\vartheta_i^*(x)}}\Big(\zeta_i^2\eta_i + \wp_2 \\ &- \frac{T^{\vartheta_i^*(x)}}{\Gamma(\vartheta_i^*(x)+1)}(\frac{\eta_i\zeta_i^1 T^\alpha}{\Gamma(\alpha+1)} + \wp_1))\Big)\Big\}. \end{aligned}$$

From (19), we have $\mathbb{T}_i\mathbb{S}_{\eta_i} \subset \mathbb{S}_{\eta_i}$. Also, we can assume that $\mathbb{Y}_i, \mathcal{U}_i \in \mathbb{C}([0,1],\mathbb{R}_e)$, $k \geq 1$

for $x \geq s \in [0,1]$, one gets

$$
\begin{aligned}
&|\mathbb{T}_i\mathbb{Y}_i(x) - \mathbb{T}_i\mathcal{U}_i(x)| = \Big|\frac{1}{\Gamma(\vartheta_i^*(x))}\int_0^x (x-s)^{\vartheta_i^*(x)-1}\mathcal{H}_i(s, \frac{1}{\Gamma(\alpha)}\int_0^s (s-r)^{\alpha-1}\mathbb{Y}_i(r)dr)ds \\
&+ \frac{x^{1-\vartheta_i^*(x)}}{\ell^{1-\vartheta_i^*(x)}}\Big(\mathcal{P}_i(x, \mathbb{Y}_i(x)) - \frac{1}{\Gamma(\vartheta_i^*(x))}\int_0^l (l-s)^{\vartheta_i^*(x)-1}\mathcal{H}_i(s, \frac{1}{\Gamma(\alpha)}\int_0^s (s-r)^{\alpha-1}\mathbb{Y}_i(r)dr)ds\Big) \\
&- \Big[\frac{1}{\Gamma(\vartheta_i^*(x))}\int_0^x (x-s)^{\vartheta_i^*(x)-1}\mathcal{H}_i(s, \frac{1}{\Gamma(\alpha)}\int_0^s (s-r)^{\alpha-1}\mathcal{U}_i(r)dr)ds + \frac{x^{1-\vartheta_i^*(x)}}{\ell^{1-\vartheta_i^*(x)}}\Big(\mathcal{P}_i(x,\mathcal{U}_i(x)) \\
&- \frac{1}{\Gamma(\vartheta_i^*(x))}\int_0^l (l-s)^{\vartheta_i^*(x)-1}\mathcal{H}_i(s, \frac{1}{\Gamma(\alpha)}\int_0^s (s-r)^{\alpha-1}\mathcal{U}_i(r)dr)ds\Big)\Big]\Big| \\
&\leq \frac{1}{\Gamma(\vartheta_i^*(x))}\int_0^x (x-s)^{\vartheta_i^*(x)-1}\big|\mathcal{H}_i(s, \frac{1}{\Gamma(\alpha)}\int_0^s (s-r)^{\alpha-1}\mathbb{Y}_i(r)dr)ds - \mathcal{H}_i(s, \frac{1}{\Gamma(\alpha)}\int_0^s (s-r)^{\alpha-1}\mathcal{U}_i(r)dr)ds\big| \\
&+ \frac{x^{1-\vartheta_i^*(x)}}{\ell^{1-\vartheta_i^*(x)}}\Big(\big|\mathcal{P}_i(x, \mathbb{Y}_i(x)) - \mathcal{P}_i(x,\mathcal{U}_i(x))\big| \\
&- \frac{1}{\Gamma(\vartheta_i^*(x))}\int_0^l (l-s)^{\vartheta_i^*(x)-1}\big|\mathcal{H}_i(s, \frac{1}{\Gamma(\alpha)}\int_0^s (s-r)^{\alpha-1}\mathbb{Y}_i(r)dr)ds - \mathcal{H}_i(s, \frac{1}{\Gamma(\alpha)}\int_0^s (s-r)^{\alpha-1}\mathcal{U}_i(r)dr)ds\big|\Big) \\
&\leq \Big[\frac{T^{\vartheta_i^*(x)}}{\Gamma(\vartheta_i^*(x)+1)}\frac{\zeta_i^1 T^\alpha}{\Gamma(\alpha+1)} + \frac{x^{1-\vartheta^*(x)}}{l^{1-\vartheta_i^*(x)}}\Big(\zeta_2^i - \frac{l^{\vartheta_i^*(x)}}{\Gamma(\vartheta_i^*(x+1))}\frac{\zeta_i^1 T^\alpha}{\Gamma(\alpha+1)}\Big)\Big]\|\mathbb{Y}_i - \mathcal{U}_i\| \\
&\leq \mathcal{H}_i|\mathbb{Y}_i - \mathcal{U}_i|.
\end{aligned}
$$

For $\mathcal{H}_i < 1$, given by (16), the $\mathbb{T}_i$ is contraction and applying the Banach's FPT [43] implies the VO-ID-system (10) has a unique solution.

Theorem 2. *Witht the consideration of* (H_1)*, then the VO-ID-system* (10) *has a solution.*

Proof. With the help of Theorem 1, we have that $\mathbb{T}_i$ are bounded, for $i = 1, 2, 3, \dots, n$. Let x_1, $x_2 \in [0, k]$ such that $x_2 > x_1$, and $k \leq 1$, then we have

$$
\begin{aligned}
|\mathbb{T}_i\mathbb{Y}_i(x_2) - \mathbb{T}_i\mathbb{Y}_i(x_1)| = &\Big|\frac{1}{\Gamma(\vartheta_i^*(x_2))}\int_0^{x_2} (x_2-s)^{\vartheta_i^*(x_2)-1}\mathcal{H}_i(s, \frac{1}{\Gamma(\alpha)}\int_0^s (s-r)^{\alpha-1}\mathbb{Y}_i(r)dr)ds \\
&+ \frac{x_2^{1-\vartheta_i^*(x_2)}}{\ell^{1-\vartheta_i^*(x_2)}}\Big(\mathcal{P}_i(x_2, \mathbb{Y}_i(x_2)) - \frac{1}{\Gamma(\vartheta_i^*(x_2))}\int_0^l (l-s)^{\vartheta_i^*(x_2)-1}\mathcal{H}_i(s, \frac{1}{\Gamma(\alpha)}\int_0^s (s-r)^{\alpha-1}\mathbb{Y}_i(r)dr)ds\Big) \\
&- \Big[\frac{1}{\Gamma(\vartheta_i^*(x_1))}\int_0^{x_1} (x_1-s)^{\vartheta_i^*(x_1)-1}\mathcal{H}_i(s, \frac{1}{\Gamma(\alpha)}\int_0^s (s-r)^{\alpha-1}\mathbb{Y}_i(r)dr)ds \\
&+ \frac{x_1^{1-\vartheta_i^*(x_1)}}{\ell^{1-\vartheta_i^*(x_1)}}\Big(\mathcal{P}_i(x_1, \mathbb{Y}_i(x_1)) - \frac{1}{\Gamma(\vartheta_i^*(x_1))}\int_0^l (l-s)^{\vartheta_i^*(x_1)-1}\mathcal{H}_i(s, \frac{1}{\Gamma(\alpha)}\int_0^s (s-r)^{\alpha-1}\mathbb{Y}_i(r)dr)ds\Big)\Big| \\
&\leq \Big|\frac{x_2^{\vartheta_i^*(x_2)}}{\Gamma(\vartheta_i^*(x_2)+1)} - \frac{x_1^{\vartheta_i^*(x_1)}}{\Gamma(\vartheta_i^*(x_1)+1)}\Big|\big(\frac{\eta_i\zeta_i^1 T^\alpha}{\Gamma(\alpha+1)} + \wp_1\big) \qquad (19) \\
&+ \Big|\frac{x_2^{1-\vartheta_i^*(x_2)}}{\ell^{1-\vartheta_i^*(x_2)}} - \frac{x_1^{1-\vartheta_i^*(x_1)}}{\ell^{1-\vartheta_i^*(x_1)}}\Big|\Big(\big|\mathcal{P}_i(x_2, \mathbb{Y}_i(x_2)) - \mathcal{P}_i(x_1, \mathbb{Y}_i(x_1))\big|
\end{aligned}
$$

$$+\,(\frac{\eta_i\zeta_i^1 T^\alpha}{\Gamma(\alpha+1)}+\wp_1)\Big|\frac{l^{\vartheta_i^*(x_2)}}{\Gamma(\vartheta_i^*(x_2)+1)}-\frac{l^{\vartheta_i^*(x_1)}}{\Gamma(\vartheta_i^*(x_1)+1)}\Big|\Big).$$

From (19), as $x_2 \to x_1$, then $\mathbb{T}_i\mathbb{Y}_i(x_2) \to \mathbb{T}_i\mathbb{Y}_i(x_1)$. This implies the equicontinuity of $\mathbb{T}_i$'s for all $i = 1, 2, \dots, n$. Also, for $\mathbb{Y}_i \in \{\mathbb{Y} \in \mathbb{C}([0,k], \mathbb{R}_e) : \mathbb{Y} = \hbar\mathbb{T}_i(\mathbb{Y}),\ for \hbar \in [0,1]\}$, one can get

$$\begin{aligned}
\|\mathbb{Y}_i\| &= \max_{x\in[0,T]}|\mathbb{T}_i\mathbb{Y}_i(x)| = \max_{x\in[0,T]}\Big|\frac{1}{\Gamma(\vartheta_i^*(x))}\int_0^x (x-s)^{\vartheta_i^*(x)-1}\mathcal{H}_i(s,\frac{1}{\Gamma(\alpha)}\int_0^s (s-r)^{\alpha-1}\mathbb{Y}_i(r)dr)ds\\
&+ \frac{x^{1-\vartheta_i^*(x)}}{\ell^{1-\vartheta_i^*(x)}}\Big(\mathcal{P}_i(x,\mathbb{Y}_i(x)) - \frac{1}{\Gamma(\vartheta_i^*(x))}\int_0^l (l-s)^{\vartheta_i^*(x)-1}\mathcal{H}_i(s,\frac{1}{\Gamma(\alpha)}\int_0^s (s-r)^{\alpha-1}\mathbb{Y}_i(r)dr)ds\Big)\Big|\\
&\le \Big|\frac{1}{\Gamma(\vartheta_i^*(x))}\int_0^x (x-s)^{\vartheta_i^*(x)-1}(\frac{\eta_i\zeta_i^1T^\alpha}{\Gamma(\alpha+1)}+\wp_1))ds + \frac{x^{1-\vartheta_i^*(x)}}{\ell^{1-\vartheta_i^*(x)}}\Big(\zeta_i^2\eta_i+\wp_2\\
&- \frac{1}{\Gamma(\vartheta_i^*(x))}\int_0^l (l-s)^{\vartheta_i^*(x)-1}(\frac{\eta_i\zeta_i^1T^\alpha}{\Gamma(\alpha+1)}+\wp_1))ds\Big) \qquad (20)\\
&\le \max_{x\in[0,T]}\Big\{\frac{T^{\vartheta_i^*(x)}}{\Gamma(\vartheta_i^*(x)+1)}(\frac{\|\mathbb{Y}_i\|\zeta_i^1T^\alpha}{\Gamma(\alpha+1)}+\wp_1)) + \frac{x^{1-\vartheta_i^*(x)}}{\ell^{1-\vartheta_i^*(x)}}\Big(\zeta_i^2\|\mathbb{Y}_i\|+\wp_2\\
&- \frac{T^{\vartheta_i^*(x)}}{\Gamma(\vartheta_i^*(x)+1)}(\frac{\|\mathbb{Y}_i\|\zeta_i^1T^\alpha}{\Gamma(\alpha+1)}+\wp_1)\Big)\Big\}\\
&= \Delta_{i\,1}^* + \Delta_{i\,2}^*\|\mathbb{Y}_i\|,
\end{aligned}$$

where

$$\Delta_{i\,1}^* = \max_{x\in[0,T]}\Big\{\frac{T^{\vartheta_i^*(x)}}{\Gamma(\vartheta_i^*(x)+1)}\wp_1 + \frac{x^{1-\vartheta_i^*(x)}}{\ell^{1-\vartheta_i^*(x)}}\Big(\wp_2 - \frac{T^{\vartheta_i^*(x)}}{\Gamma(\vartheta_i^*(x)+1)}\wp_1\Big)\Big\}, \qquad (21)$$

and

$$\Delta_{i\,2}^* = \max_{x\in[0,T]}\Big\{\frac{T^{\vartheta_i^*(x)}}{\Gamma(\vartheta_i^*(x)+1)}\frac{\zeta_i^1T^\alpha}{\Gamma(\alpha+1)} + \frac{x^{1-\vartheta_i^*(x)}}{\ell^{1-\vartheta_i^*(x)}}\Big(\zeta_i^2\frac{T^{\vartheta_i^*(x)}}{\Gamma(\vartheta_i^*(x)+1)}\frac{\zeta_i^1T^\alpha}{\Gamma(\alpha+1)}\Big)\Big\}. \qquad (22)$$

From (20), (21) and (22), we have

$$\|\mathbb{Y}_i\| \le \frac{\Delta_{i\,1}^*}{1-\Delta_{i\,2}^*}, \qquad (23)$$

for $i = 1, 2, \dots, n$. Thus, Leray-Schauder's alternative theorem implies that the VO-ID-system (10) has a solution.

4. Hyers-Ulam Stability

When it comes to the study of functional equations, the concept of HUS, is extremely important since it ensures that solutions remain relatively similar to the initial solution even when only minute adjustments are made. According to the assertion, if a function can produce an approximation of a solution to a particular functional equation, then there must be an exact solution located in close proximity to the approximation of the solution. The HUS theorem is useful in a number of different domains, including the branch of research devoted to FDEs. The concept of HUS is highly significant in FDEs because it provides us with a fundamental method for determining how stable solutions with fractional orders are. The stability data give confidence that minute modifications in the initial values or parameters do not result in large variations in the solutions, hence guaranteeing the precision and predictability of the system's dynamical behavior. The use of the HUS idea in FDEs is of critical significance in the study of physics, engineering, and finance, respectively. These areas of study frequently make use of fractional-order models in order to effectively represent processes that are complex and memory-dependent. The utilization of this notion makes it possible to conduct research on extended temporal patterns, the influence of memory on occurrences, and the coexistence of several scales in a variety of real-world phenomena. In addition to this, researchers are now able to define the stability characteristics of control systems with fractional order, which has important significance in the disciplines of electrical circuits, robotics, and biomedical engineering. For details, see the works i.

The HUS for the VO-ID-system (10) is defined and analyzed below.

Definition 5. *By the HUS of the* (15)*, we mean that for* $\zeta_i > 0$*, there exist* $\Delta_i > 0$*, with* $\mathbb{Y}_i$ *such that*

$$\|\mathbb{Y}_i - \mathbb{T}_i\mathbb{Y}_i\|_1 < \Delta_i, \tag{24}$$

with $\bar{\mathbb{Y}}_i(t)$ *approximations of the VO-system* (15)*, such that*

$$\bar{\mathbb{Y}}_i(t) = \mathbb{T}_i\bar{\mathbb{Y}}_i(t), \tag{25}$$

implies that

$$\|\mathbb{Y}_i - \bar{\mathbb{Y}}_i\| < \Delta_i\zeta_i, \tag{26}$$

where $i = 1, 2, \dots, n$.

Theorem 3. *Let the assumptions of* (H_1) *hold true, then our presumed VO system of FDEs* (15) *is HU stable which implies the stability of the coupled system* (10)*.*

Proof. Let for $\mathbb{Y}_i \in \mathbb{B}$ with the property (24) and an approximation $\mathcal{Y} \in \mathbb{B}$ of (10), satisfying (15), implies that

$$\begin{aligned}
|\mathbb{T}_i\mathbb{Y}_i(x) - \mathbb{T}_i\mathcal{Y}_i(x)| &= \Big|\frac{1}{\Gamma(\vartheta_i^*(x))}\int_0^x (x-s)^{\vartheta_i^*(x)-1}\mathcal{H}_i(s, \frac{1}{\Gamma(\alpha)}\int_0^s (s-r)^{\alpha-1}\mathbb{Y}_i(r)dr)ds \\
+ \quad & \frac{x^{1-\vartheta_i^*(x)}}{\ell^{1-\vartheta_i^*(x)}}\Big(\mathcal{P}_i(x, \mathbb{Y}_i(x)) - \frac{1}{\Gamma(\vartheta_i^*(x))}\int_0^l (l-s)^{\vartheta_i^*(x)-1}\mathcal{H}_i(s, \frac{1}{\Gamma(\alpha)}\int_0^s (s-r)^{\alpha-1}\mathbb{Y}_i(r)dr)ds\Big) \\
- \quad & \Big[\frac{1}{\Gamma(\vartheta_i^*(x))}\int_0^x (x-s)^{\vartheta_i^*(x)-1}\mathcal{H}_i(s, \frac{1}{\Gamma(\alpha)}\int_0^s (s-r)^{\alpha-1}\mathcal{Y}_i(r)dr)ds + \frac{x^{1-\vartheta_i^*(x)}}{\ell^{1-\vartheta_i^*(x)}}\Big(\mathcal{P}_i(x, \mathcal{Y}_i(x))
\end{aligned}$$

$$
\begin{aligned}
&- \frac{1}{\Gamma(\vartheta_i^*(x))}\int_0^l (l-s)^{\vartheta_i^*(x)-1}\mathcal{H}_i(s,\frac{1}{\Gamma(\alpha)}\int_0^s (s-r)^{\alpha-1}\mathcal{Y}_i(r)dr)ds\Big)\Big]\Big| \qquad (27)\\
&\leq \frac{1}{\Gamma(\vartheta_i^*(x))}\int_0^x (x-s)^{\vartheta_i^*(x)-1}\big|\mathcal{H}_i(s,\frac{1}{\Gamma(\alpha)}\int_0^s (s-r)^{\alpha-1}\mathbb{Y}_i(r)dr)ds - \mathcal{H}_i(s,\frac{1}{\Gamma(\alpha)}\int_0^s (s-r)^{\alpha-1}\mathcal{Y}_i(r)dr)ds\big|\\
&+ \frac{x^{1-\vartheta_i^*(x)}}{\ell^{1-\vartheta_i^*(x)}}\Big(\big|\mathcal{P}_i(x,\mathbb{Y}_i(x)) - \mathcal{P}_i(x,\mathcal{Y}_i(x))\big|\\
&- \frac{1}{\Gamma(\vartheta_i^*(x))}\int_0^l (l-s)^{\vartheta_i^*(x)-1}\big|\mathcal{H}_i(s,\frac{1}{\Gamma(\alpha)}\int_0^s (s-r)^{\alpha-1}\mathbb{Y}_i(r)dr)ds - \mathcal{H}_i(s,\frac{1}{\Gamma(\alpha)}\int_0^s (s-r)^{\alpha-1}\mathcal{Y}_i(r)dr)ds\big|\Big)\\
&\leq \Big[\frac{T^{\vartheta_i^*(x)}}{\Gamma(\vartheta_i^*(x)+1)}\frac{\zeta_i^1 T^\alpha}{\Gamma(\alpha+1)} + \frac{x^{1-\vartheta^*(x)}}{l^{1-\vartheta_i^*(x)}}\Big(\zeta_2^i - \frac{l^{\vartheta_i^*(x)}}{\Gamma(\vartheta_i^*(x+1))}\frac{\zeta_i^1 T^\alpha}{\Gamma(\alpha+1)}\Big)\Big]\|\mathbb{Y}_i - \mathcal{Y}_i\|\\
&\leq \mathcal{H}_i|\mathbb{Y}_i - \mathcal{Y}_i|.
\end{aligned}
$$

For $\mathcal{H}_i < 1$, where $\mathcal{H}_i = \max_{x\in[0,T]}\big\{\frac{T^{\vartheta_i^*(x)}}{\Gamma(\vartheta_i^*(x)+1)}\frac{\zeta_i^1 T^\alpha}{\Gamma(\alpha+1)} + \frac{x^{1-\vartheta^*(x)}}{l^{1-\vartheta_i^*(x)}}\Big(\zeta_2^i - \frac{l^{\vartheta_i^*(x)}}{\Gamma(\vartheta_i^*(x+1))}\frac{\zeta_i^1 T^\alpha}{\Gamma(\alpha+1)}\Big)\big\}$ for $i = 1, 2, \ldots, n$. From (24), (25) and (27), we have

$$
\begin{aligned}
\|\mathbb{Y}_i - \mathcal{Y}_i\| &= \|\mathbb{Y}_i - \mathbb{T}_i\mathbb{Y}_i + \mathbb{T}_i\mathbb{Y}_i - \mathcal{Y}_i\|\\
&\leq \|\mathbb{Y}_i - \mathbb{T}_i\mathbb{Y}_i\| + \|\mathbb{T}_i\mathbb{Y}_i - \mathbb{T}_i\mathcal{Y}\| \qquad (28)\\
&\leq \Delta_i + \mathcal{H}_i\|\mathbb{Y}_i - \mathcal{Y}_i\|,
\end{aligned}
$$

where $i = 1, 2, \ldots, m$. Furthermore,

$$
\|\mathbb{Y}_i - \mathcal{Y}_i\| \leq \frac{\Delta_i}{1-\mathcal{H}_i}, \qquad (29)
$$

with $\zeta_i = \frac{1}{1-\mathcal{H}_i}$. Hence, (15) is HU-stable, equivalently; the HUS of (10) is proved.

5. Numerical technique

In numerical analysis, there are so many ways to handle the integration of nonlinear functions. Lagrange's interpolation (LI) polynomial is one of them which is used in diverse fields for different applications. The Lagrange interpolation polynomial is a widely utilized mathematical technique that has applications in many academic disciplines such as mathematics, computer science, engineering, and data analysis. The approach described enables the estimation of an intricate function by generating a polynomial that intersects a predetermined set of data points. LI holds significant importance within the field of numerical analysis in mathematics. The utilization of an interpolating polynomial greatly facilitates the task of determining a polynomial function that accurately represents a given dataset. This, in turn, allows for the estimation of values that lie between the existing data points with a high degree of precision. This methodology is utilized in the fields of calculus, differential equations, and numerical integration. LI plays a crucial role in the fields of data compression and error correction within the realm of computer science. The utilization of this technique is prevalent in the fields of image and signal processing, as it plays a crucial role in the precise reconstruction of data that is either absent or distorted. Additionally, it assumes a prominent function in the realm of computer graphics by facilitating the generation of seamless curves and surfaces derived from limited data points.

Here, we develop an iterative scheme for the numerical simulations of (10). We consider

$$\begin{aligned}\mathbb{T}_i\mathbb{Y}_i(x) &= \frac{1}{\Gamma(\vartheta_i^*(x))}\int_0^x (x-s)^{\vartheta_i^*(x)-1}\mathcal{H}_i(s,\frac{1}{\Gamma(\alpha)}\int_0^s (s-r)^{\alpha-1}\mathbb{Y}_i(r)dr)ds + \frac{x^{1-\vartheta_i^*(x)}}{\ell^{1-\vartheta_i^*(x)}}\Big(\mathcal{P}_i(x,\mathbb{Y}_i(x))\\ &- \frac{1}{\Gamma(\vartheta_i^*(x))}\int_0^l (l-s)^{\vartheta_i^*(x)-1}\mathcal{H}_i(s,\frac{1}{\Gamma(\alpha)}\int_0^s (s-r)^{\alpha-1}\mathbb{Y}_i(r)dr)ds\Big). \end{aligned} \tag{30}$$

We assume the nonlinear function $\mathcal{G}_i^*(x,\mathbb{Y}_i(x)) = \mathcal{H}_i(s,\frac{1}{\Gamma(\alpha)}\int_0^s (s-r)^{\alpha-1}\mathbb{Y}_i(r)dr)$. Then, (30) becomes

$$\begin{aligned}\mathbb{T}_i\mathbb{Y}_i(x) &= \frac{1}{\Gamma(\vartheta_i^*(x))}\int_0^x (x-s)^{\vartheta_i^*(x)-1}\mathcal{G}_i^*(s,\mathbb{Y}_i(s))ds + \frac{x^{1-\vartheta_i^*(x)}}{\ell^{1-\vartheta_i^*(x)}}\Big(\mathcal{P}_i(x,\mathbb{Y}_i(x)) \qquad (31)\\ &- \frac{1}{\Gamma(\vartheta_i^*(x))}\int_0^l (l-s)^{\vartheta_i^*(x)-1}\mathcal{G}_i^*(s,\mathbb{Y}_i(s))ds\Big).\end{aligned}$$

Replacing x by x_{k+1} in (31), we get the following discretization of the integral system

$$\begin{aligned}\mathbb{T}_i\mathbb{Y}_i(x_{k+1}) &= \frac{1}{\Gamma(\vartheta_i^*(x_k))}\sum_{m=0}^{m=k}\int_{x_m}^{x_{m+1}} (x_k-s)^{\vartheta_i^*(x_k)-1}\mathcal{G}_i^*(s,\mathbb{Y}_i(s))ds \qquad (32)\\ &+ \frac{x_k^{1-\vartheta_i^*(x_k)}}{\ell^{1-\vartheta_i^*(x_k)}}\Big(\mathcal{P}_i(x_k,\mathbb{Y}_i(x_k)) - \frac{1}{\Gamma(\vartheta_i^*(x_k))}\int_0^l (l-s)^{\vartheta_i^*(x_k)-1}\mathcal{G}_i^*(s,\mathbb{Y}_i(s))ds\Big).\end{aligned}$$

With the help of LIP, we can approximate the nonlinear function $\mathcal{G}_i^*(x,\mathbb{Y}_i(x))$ as below:

$$\begin{aligned}\mathcal{G}_i^*(x,\mathbb{Y}_i(x)) &= \frac{\mathcal{G}_i^*(x_m,\mathbb{Y}_i(x_m))(x-x_{m-1})}{x_m-x_{m-1}} - \frac{\mathcal{G}_i^*(x_{m-1},\mathbb{Y}_i(x_{m-1}))(x-x_m)}{x_m-x_{m-1}} \qquad (33)\\ &= \frac{\mathcal{G}_i^*(x_m,\mathbb{Y}_i(x_m))(x-x_{m-1})}{\hbar} - \frac{\mathcal{G}_i^*(x_{m-1},\mathbb{Y}_i(x_{m-1}))(x-s_m)}{\hbar}.\end{aligned}$$

The (33) leads us to the following numerical scheme

$$\begin{aligned}\mathbb{Y}_i(x_{k+1}) = &\frac{h^{\vartheta_i^*(x_k)}}{\Gamma(\vartheta_i^*(x_k)+2)}\Sigma_{m=0}^k\Big[\mathcal{G}_i^*(x_m,\mathbb{Y}_i(x_m))\Big((k-m+1)^{\vartheta_i^*(x_m)}(2+k-m+\vartheta_i^*(x_m))\\ &-(k-m)^{\varrho_i}(k+2-m+2\vartheta_i^*(x_m))\Big) \qquad (34)\\ &-\mathcal{G}_i^*(x_{m-1},\mathbb{Y}_i(x_{m-1}))\Big((k-m+1)^{\vartheta_i^*(x_{m-1})+1}-(k-m+1+\vartheta_i^*(x_{m-1}))(k-m)^{\vartheta_i^*(x_{m-1})}\Big)\Big]\\ &+\frac{x_m^{1-\vartheta_i^*(x_m)}}{\ell^{1-\vartheta_i^*(x_m)}}\Big(\sum_{i=0}^n\mathcal{P}_i(x_k,\mathbb{Y}_i(x_k)) - \Sigma_{k=1}^m\Big[\frac{\mathcal{G}_i^*(x_k,\mathbb{Y}_i(x_k))}{h}\Big(\frac{x_k\ell^{\vartheta_i^*(x_k)}}{\Gamma(\vartheta_i^*(x_k)+1)} - \frac{\ell^{\vartheta_i^*(x_k+1)}}{\Gamma(\vartheta_i^*(x_k)+2)}\Big)\end{aligned}$$

$$- \frac{\mathcal{G}_i^*(x_{k-1}, \mathbb{Y}_i(x_{k-1}))}{h} \left(\frac{x_k \ell^{\vartheta_i^*(x_k)}}{\Gamma(\vartheta_i^*(x_k)+1)} - \frac{\ell^{\vartheta_i^*(x_k+1)}}{\Gamma(\vartheta_i^*(x_k)+2)} \right) \Bigg) \Bigg],$$

here, $m,\ k \in \{1, 2, \ldots, n\}$.

5.1. Chaotic power system

In this section, we are utilizing the computational scheme (34) for the numerical study of a power system model. The dynamics of the power system are provided as a fractional order extension of the model in [33]:

$$\begin{aligned}
\mathbb{D}^{\vartheta}\delta_m &= w_s,\\
\mathbb{D}^{\vartheta}w_s &= 16.6667\sin(\delta - \delta_m + 0.0873)\nu - 0.1667w_s + 1.8807 + d_2,\\
\mathbb{D}^{\vartheta}\delta\ &= 496.8718\nu^2 - 166.6667\cos(\delta - \delta_m - 0.0873)\nu\\
&\quad -666.6667\cos(\delta - 0.2094)\nu - 93.3333\nu + 33.3333\mathcal{Q} + 43.333,\\
\mathbb{D}^{\vartheta}\nu\ &= -78.7638\nu^2 + 26.2172\cos(\delta - \delta_m - 0.0124)\nu\\
&\quad +104.8689\cos(\delta - 0.1346)\nu + 14.5229\nu - 5.2288\mathcal{Q} - 7.0327 + d_4,
\end{aligned} \tag{35}$$

where $\mathcal{Q} = 11.377$. Here, $\delta_m = 0.4$ denotes the generator power angle; $\delta = 0.2$ and $\nu = 0.97$ are phase angle and amplitude; Q_1 is the load of power; $w_s = 0$ denotes the generator frequency deviation. The explanation of the model can be further studied in [33, 35].

Therefore, phase trajectories of the nonlinear power system are shown in Figure 1.

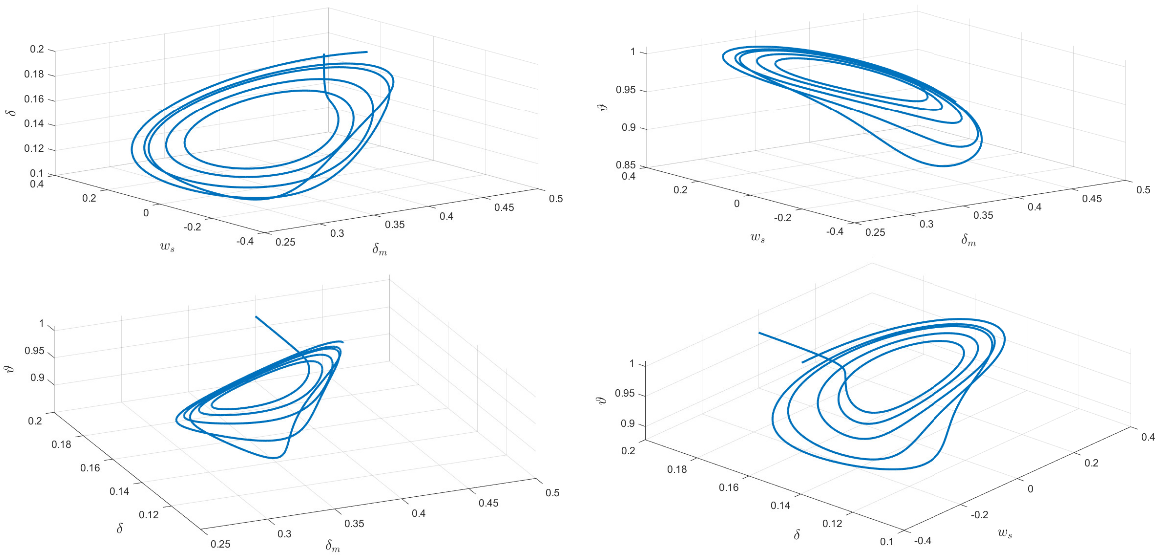

Figure 1: Three-dimensional phase trajectories of nonlinear power system

6. Control Development

The present study examines the nonlinear dynamics of power systems. The presented mathematical model is being analyzed as a means of understanding the behavior of robust control and stability of the system.

$$\mathbb{D}^{\vartheta} y_i = f_i(y,t) + u_i(t) + d_i(t) \tag{36}$$

where $|d(t)| \leq \xi$, and it is unknown constant $\xi > 0$.
To calculate the tracking error, one can use the expression as $e_i(t) = y_i(t) - y_{di}(t)$ and $\mathbb{D}^{\vartheta} e_i(t) = \mathbb{D}^{\vartheta} y_i(t) - \mathbb{D}^{\vartheta} y_{di}(t)$,

$$\mathbb{D}^{\vartheta} e_i(t) = f_i(y,t) + u_i(t) + d_i(t) - \mathbb{D}^{\vartheta} y_{di}(t) \tag{37}$$

6.1. Fixed-time fractional-order SMC

The utilization of sliding surfaces in fixed-time represents a feasible approach for achieving rapid and efficient convergence while simultaneously minimizing control input chattering. In order to enhance the efficiency of the sliding mode control, the integration of fractional-order control can be considered. This work presents a potential solution in the form of a fractional-order with fixed-time sliding mode control. Therefore, the fractional-order sliding surface that is being suggested is expressed as

$$S_i = \mathbb{D}^{\vartheta-1} e_i + k_1 \mathbb{D}^{\vartheta-2} |e_i|^{p_1} sign(e_i) + k_2 \mathbb{D}^{\vartheta-2} |e_i|^{p_2} sign(e_i) \tag{38}$$

where k_1, k_2 are positive constants, $0 < \vartheta, p_1 < 1$ and $p_2 > 1$. And its derivative is obtained as

$$\dot{S}_i = \mathbb{D}^{\vartheta} e_i + k_1 \mathbb{D}^{\vartheta-1} |e_i|^{p_1} sign(e_i) + k_2 \mathbb{D}^{\vartheta-1} |e_i|^{p_2} sign(e_i) \tag{39}$$

The substitution of the error (37) into equation (39), we get

$$\begin{aligned} &\dot{S}_i = f_i(y,t) + u_i + d_i - \mathbb{D}^{a} y_{id} \\ &+ k_1 \mathbb{D}^{\vartheta-1} |e_i|^{p_1} sign(e_i) + k_2 \mathbb{D}^{\vartheta-1} |e_i|^{p_2} sign(e_i) \end{aligned} \tag{40}$$

Following that, a fractional sliding mode control strategy is implemented through the development of a suitable fractional-order sliding surface. This design ensures that the error paths effectively converge to the sliding surface within a fixed time and remain on it. In order to guarantee the convergence and stability with established dynamics, a fixed-time fractional-order sliding mode control system is constructed as

$$\begin{aligned} &u_i = -f_i(y,t) - \xi_i sign(S_i) + \mathbb{D}^{\vartheta} y_{id} \\ &- k_1 \mathbb{D}^{\vartheta-1} |e_i|^{p_1} sign(e_i) - k_2 \mathbb{D}^{\vartheta-1} |e_i|^{p_2} sign(e_i) \\ &- \mathcal{K}_1 |S_i|^{q_1} sign(S_i) - \mathcal{K}_2 |S_i|^{q_2} sign(S_i) \end{aligned} \tag{41}$$

where $\mathcal{K}_1$ and $\mathcal{K}_2$ are positive constants, $0 < q_1 < 1$ and $q_2 > 1$. Therefore, the substitution of control input (41) into (40), one can have

$$\dot{S}_i = d_i - \xi_i sign(S_i) - \mathcal{K}_1 |S_i|^{q_1} sign(S_i) - \mathcal{K}_2 |S_i|^{q_2} sign(S_i) \tag{42}$$

Theorem 4. *By considering the dynamics described in equation (36), it is evident that the trajectories of the system converge to the origin within a fixed time.*

Proof: The preferred equation of the Lyapunov function is described below

$$V_1 = 0.5 \sum_{i=1}^{n} {e_i}^2 \tag{43}$$

This can also be derived and written as

$$\dot{V}_1 = \sum_{i=1}^{n} e_i \dot{e}_i = \sum_{i=1}^{n} e_i \mathbb{D}^{1-\vartheta}(\mathbb{D}^{\vartheta} e_i) \tag{44}$$

If $S = \dot{S} = 0$, one can obtain

$$\mathbb{D}^{\vartheta} e_i = -k_1 \mathbb{D}^{\vartheta-1}|e_i|^{p_1} sign(e_i) - k_2 \mathbb{D}^{\vartheta-1}|e_i|^{p_2} sign(e_i) \tag{45}$$

Equation (46) is obtained by substituting (45) into (44) as

$$\dot{V}_1 = \sum_{i=1}^{n} e_i \mathbb{D}^{1-\vartheta}(-k_1 \mathbb{D}^{\vartheta-1}|e_i|^{p_1} sign(e_i) - k_2 \mathbb{D}^{\vartheta-1}|e_i|^{p_2} sign(e_i)) \tag{46}$$

It can be simplified as

$$\begin{aligned} \dot{V}_1 &= -k_1 \sum_{i=1}^{n} |e_i|^{p_1+1} - k_2 \sum_{i=1}^{n} |e_i|^{p_2+1} \\ &= -k_1 \sum_{i=1}^{n} \left(|e_i|^2\right)^{\frac{p_1+1}{2}} - k_2 \sum_{i=1}^{n} \left(|e_i|^2\right)^{\frac{p_2+1}{2}} \end{aligned} \tag{47}$$

According to Lemma 2, one can express as

$$\dot{V}_1 \le -k_1 \left(\sum_{i=1}^{n} |e_i|^2\right)^{\frac{p_1+1}{2}} - k_2 n^{\frac{1-p_2}{2}} \left(\sum_{i=1}^{n} |e_i|^2\right)^{\frac{p_2+1}{2}} \tag{48}$$

And (48) can be rewritten as

$$\dot{V}_1 \le -k_1 2^{\frac{p_1+1}{2}} V_1^{\frac{p_1+1}{2}} - k_2 n^{\frac{1-p_2}{2}} 2^{\frac{p_2+1}{2}} V_1^{\frac{p_2+1}{2}} \tag{49}$$

The fixed settling time is calculated with Lemma 1 as

$$T_s = \frac{2}{k_1 2^{\frac{p_1+1}{2}}(1-p_1)} + \frac{2}{k_2 n^{\frac{1-q_1}{2}} 2^{\frac{p_2+1}{2}}(p_2-1)} \tag{50}$$

Therefore, it is established that the tracking error will ultimately approach zero in a fixed time.

Theorem 5. *Considering the nonlinear fractional system* (36) *with the error dynamics* (37)*. When the system is controlled by* (41)*, the states are converged to the sliding surface* (38) *in a fixed time.*

Proof: The suitable Lyapunov function is given as follows

$$V_2 = 0.5 \sum_{i=1}^{n} {S_i}^2 \tag{51}$$

The equation (51) can be derived as

$$\dot{V}_2 = \sum_{i=1}^{n} S_i \dot{S}_i \tag{52}$$

Equation (42) is substituted in (52), we get

$$\dot{V}_2 = \sum_{i=1}^{n} S_i \dot{S}_i = \sum_{i=1}^{n} S_i (d_i - \xi sign(S_i) - \mathcal{K}_1 |S_i|^{q_1} sign(S_i) - \mathcal{K}_2 |S_i|^{q_2} sign(S_i)) \tag{53}$$

Using the bounded condition of disturbance, we have

$$\begin{aligned} \dot{V}_2 &\leq -\mathcal{K}_1 \sum_{i=1}^{n} |S_i|^{q_1+1} - \mathcal{K}_2 \sum_{i=1}^{n} |S_i|^{q_2+1} \\ &= -\mathcal{K}_1 \sum_{i=1}^{n} \left(|S_i|^2\right)^{\frac{q_1+1}{2}} - \mathcal{K}_2 \sum_{i=1}^{n} \left(|S_i|^2\right)^{\frac{q_2+1}{2}} \end{aligned} \tag{54}$$

According to Lemma 2, (54) can be deduced as

$$\dot{V}_2 \leq -\mathcal{K}_1 \left(\sum_{i=1}^{n} |S_i|^2 \right)^{\frac{q_1+1}{2}} - \mathcal{K}_2 n^{\frac{1-q_2}{2}} \left(\sum_{i=1}^{n} |S_i|^2 \right)^{\frac{q_2+1}{2}} \tag{55}$$

And (55) can be rewritten as

$$\dot{V}_2 \leq -\mathcal{K}_1 2^{\frac{q_1+1}{2}} V_2^{\frac{q_1+1}{2}} - \mathcal{K}_2 n^{\frac{1-q_2}{2}} 2^{\frac{q_2+1}{2}} V_2^{\frac{q_2+1}{2}} \tag{56}$$

Thus, according to Lemma 1, reaching time can be formulated as

$$T_{r1} = \frac{2}{\mathcal{K}_1 2^{\frac{q_1+1}{2}} (1 - q_1)} + \frac{2}{\mathcal{K}_2 n^{\frac{1-q_2}{2}} 2^{\frac{q_2+1}{2}} (q_2 - 1)} \tag{57}$$

As a result, it can be noticed that the states of the system will ultimately approach a value of S in a fixed time. The proof has been satisfactorily completed.

6.2. Adaptive fixed-time fractional-order SMC

The equation presented below illustrates the proposed adaptive strategy utilizing fixed-time sliding mode control. The primary objective of this study is to address and overcome the unknown disturbance in the systems. The control scheme that has been suggested is presented as follows

$$\begin{aligned} u_i = &-f_i(y,t) - \hat{\xi}_i sign(S_i) + \mathbb{D}^{\vartheta} y_{id} \\ &-k_1 \mathbb{D}^{\vartheta-1}|e_i|^{p_1} sign(e_i) - k_2 \mathbb{D}^{\vartheta-1}|e_i|^{p_2} sign(e_i) \\ &-\mathcal{K}_1|S_i|^{q_1} sign(S_i) - \mathcal{K}_2|S_i|^{q_2} sign(S_i) \end{aligned} \tag{58}$$

where $\hat{\xi}$ is the estimation of ξ is given as

$$\dot{\hat{\xi}} = \varsigma|S| \tag{59}$$

with tuning parameter $\varsigma > 0$. The equation (58) is substituted in (40), we can get

$$\dot{S}_i = d_i - \hat{\xi}_i sign(S_i) - \mathcal{K}_1|S_i|^{q_1} sign(S_i) - \mathcal{K}_2|S_i|^{q_2} sign(S_i) \tag{60}$$

Theorem 6. *Consider the nonlinear fraction system* (36) *and the error* (37). *The control input* (58) *with adaptive law* (59), *the trajectories are converged to the sliding surface* (38) *in a fixed time.*

Proof: The suitable Lyapunov function is selected as follows

$$V_3 = 0.5\sum_{i=1}^{n} {S_i}^2 + \frac{0.5}{\varsigma}\tilde{\xi}^2 \tag{61}$$

where $\tilde{\xi} = \hat{\xi} - \xi$. Its derivative can be derived as

$$\dot{V}_3 = \sum_{i=1}^{n} S_i\dot{S}_i + \frac{1}{\varsigma}\tilde{\xi}\dot{\hat{\xi}} \tag{62}$$

Equation (60) is substituted in (62), $\dot{V}_3$ is computed as

$$\begin{aligned} \dot{V}_3 = &\sum_{i=1}^{n} S_i(d_i - \hat{\xi} sign(S_i) - \mathcal{K}_1|S_i|^{q_1} sign(S_i) - \mathcal{K}_2|S_i|^{q_2} sign(S_i)) \\ &+\tfrac{1}{\varsigma}\tilde{\xi}\dot{\hat{\xi}} \end{aligned} \tag{63}$$

Using (59) with disturbance bounded condition, (63) can be realized as

$$\dot{V}_3 \leq -\mathcal{K}_1\sum_{i=1}^{n}|S_i|^{q_1+1} - \mathcal{K}_2\sum_{i=1}^{n}|S_i|^{q_2+1} \tag{64}$$

It is rewritten as

$$\dot{V}_3 \leq -\mathcal{K}_1\sum_{i=1}^{n}\left(|S_i|^2\right)^{\frac{q_1+1}{2}} - \mathcal{K}_2\sum_{i=1}^{n}\left(|S_i|^2\right)^{\frac{q_2+1}{2}} \tag{65}$$

According to Lemma 2, (65) can be expressed as

$$\dot{V}_3 \leq -\mathcal{K}_1 \left(\sum_{i=1}^{n} |S_i|^2 \right)^{\frac{q_1+1}{2}} - \mathcal{K}_2 n^{\frac{1-q_2}{2}} \left(\sum_{i=1}^{n} |S_i|^2 \right)^{\frac{q_2+1}{2}} \tag{66}$$

Then (66) can be written as

$$\dot{V}_3 \leq -\mathcal{K}_1 [2(V_3 - \chi)]^{\frac{q_1+1}{2}} - \mathcal{K}_2 n^{\frac{1-q_2}{2}} [2(V_3 - \chi)]^{\frac{q_2+1}{2}} \tag{67}$$

where $\chi = \frac{0.5}{\varsigma} \tilde{\xi}^2$.

$$\dot{V}_3 \leq -\mathcal{K}_1 2^{\frac{q_1+1}{2}} \left(1 - \frac{\chi}{V_3}\right)^{\frac{q_1+1}{2}} V_3^{\frac{q_1+1}{2}} - \mathcal{K}_2 n^{\frac{1-q_2}{2}} 2^{\frac{q_2+1}{2}} \left(1 - \frac{\chi}{V_3}\right)^{\frac{q_2+1}{2}} V_3^{\frac{q_2+1}{2}} \tag{68}$$

The reaching time is obtained using Lemma 1

$$T_{r2} = \frac{2}{\Omega_1(1 - q_1)} + \frac{2}{\Omega_2(q_2 - 1)} \tag{69}$$

where $\Omega_1 = \mathcal{K}_1 2^{\frac{q_1+1}{2}} \left(1 - \frac{\chi}{V_3}\right)^{\frac{q_1+1}{2}}$, $\Omega_2 = \mathcal{K}_2 n^{\frac{1-q_2}{2}} 2^{\frac{q_2+1}{2}} \left(1 - \frac{\chi}{V_3}\right)^{\frac{q_2+1}{2}}$.

Consequently, the state trajectories will ultimately approach zero within a fixed time and the time $T = T_{r2} + T_s$ can be obtained. The proof has been completed.

7. Simulation Results of Proposed Control Method

This section provides an illustrative example to support the theoretical conclusions and demonstrate the effectiveness of the suggested adaptive fixed-time fractional sliding mode control method used to control the fractional power system. The utilization of the Matlab/Simulink software is employed for the execution of numerical simulations. The dynamics of the fractional power system are provided as:

$$\begin{aligned}
\mathbb{D}^{\vartheta}\delta_m &= w_s, \\
\mathbb{D}^{\vartheta}w_s &= 16.6667\sin(\delta - \delta_m + 0.0873)\nu - 0.1667w_s + 1.8807 + d_2 + u_2, \\
\mathbb{D}^{\vartheta}\delta &= 496.8718\nu^2 - 166.6667\cos(\delta - \delta_m - 0.0873)\nu \\
&\quad -666.6667\cos(\delta - 0.2094)\nu - 93.3333\nu + 33.3333\mathcal{Q} + 43.333, \\
\mathbb{D}^{\vartheta}\nu &= -78.7638\nu^2 + 26.2172\cos(\delta - \delta_m - 0.0124)\nu \\
&\quad +104.8689\cos(\delta - 0.1346)\nu + 14.5229\nu - 5.2288\mathcal{Q} - 7.0327 + d_4 + u_4.
\end{aligned} \tag{70}$$

where $\mathcal{Q} = 11.377$. The suitable parameters of the proposed control method are chosen as: $k_1 = 10$, $k_2 = 10$, $\mathcal{K}_1 = 10$, $\mathcal{K}_2 = 20$, $p_1 = 0.66$, $q_1 = 0.4$, $p_2 = 1.5$, $q_2 = 1.1$ and $\vartheta = 0.99$. In addition, the external disturbance is $sin(t)$, and the reference trajectories are given as $y_{d2} = 0$ and $y_{d4} = 1$. Here, $\delta_m = 0.38$ denotes the generator power angle; $\delta = 0.1$ and $\nu = 0.97$ are phase angle and amplitude; $\mathcal{Q}$ is the load of power; $w_s = 1.5$.

Therefore, the numerical results are shown of the proposed scheme with the comparison of FFoSMC [35]. Thus, states of the power system are given in Figure 2, trajectory tracking performances are depicted in Figure 3, and the comparison of control inputs is shown in Figure 4.

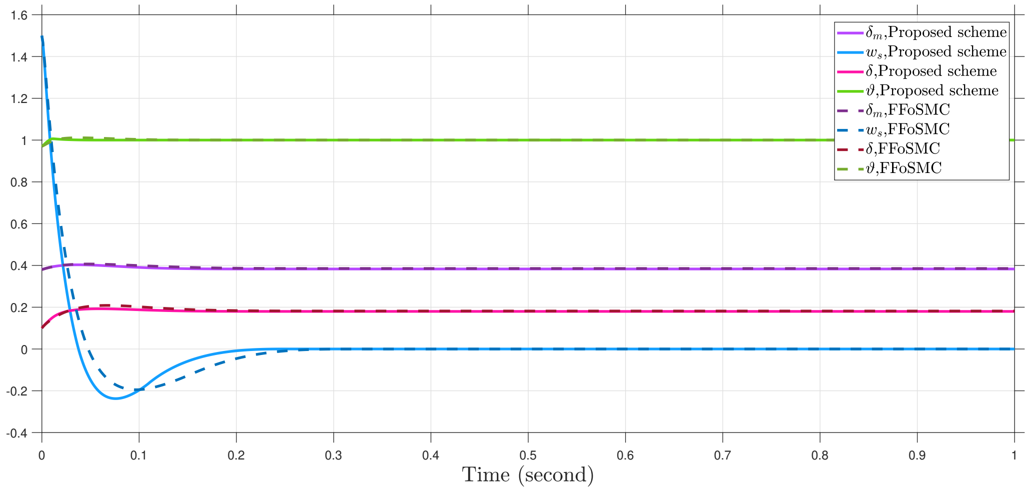

Figure 2: States trajectories

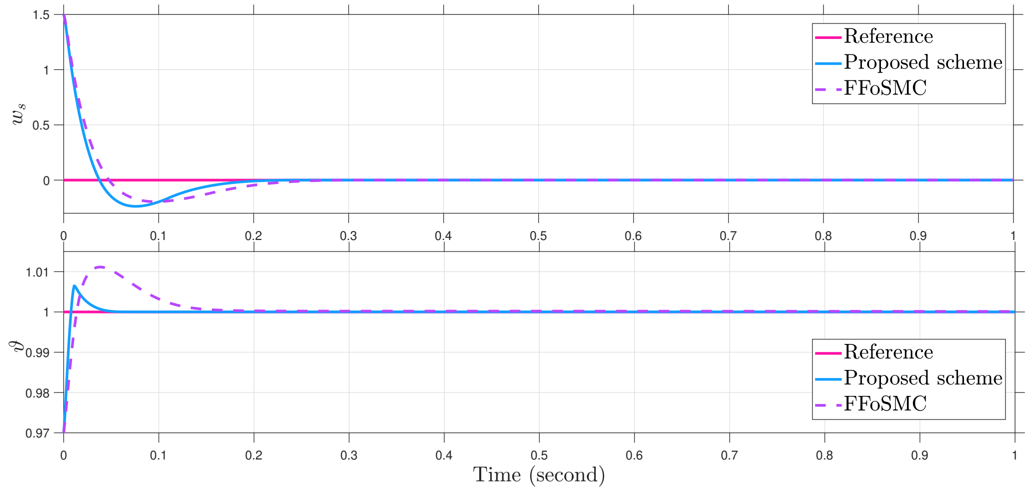

Figure 3: State trajectory tracking comparison

It can be seen from the results shown in Figure 2 that the convergence is better than the current approach FFoSMC. The findings suggest that states effectively follow their intended goals and maintain stability, thus accomplishing their objectives with the proposed scheme. The w_s and ϑ are depicted in Figure 3, which illustrates the proposed controller's ability to precisely track a reference signal in a prompt manner. Nevertheless, it is worth mentioning that the proposed approach exhibits superior performance compared to the

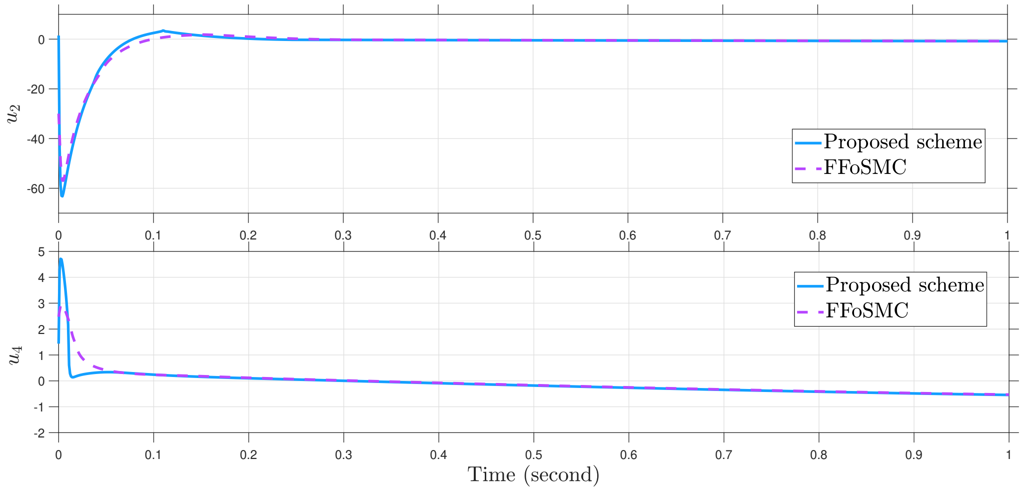

Figure 4: Control input

FFoSMC method in terms of its convergence and tracking. Based on the data derived from the simulation results, it can be inferred that the suggested controller effectively achieves the desired purpose without exhibiting any apparent issues. Furthermore, Figure 4 illustrates the comparison of control inputs between the recommended scheme and the FFoSMC scheme.

8. Discussion

This section presents a comprehensive examination of the simulated results obtained from the fractional system and controller. Additionally, this research investigates the limitations linked to the proposed controller about its parameters and stability analyses. Following this, a thorough investigation is undertaken to clarify the potential uses of the suggested approach in combination with other nonlinear systems.

Here a discussion is given for the results obtained for the system of VO-ID-system (10). Our findings include mathematical analysis and computational results. In the mathematical analysis of (10), we have started our work from the fixed point approach for which the conversion to the integral system is carried out with the help of the variable order FC which is obtained in the Lemma 3. After the integral system is obtained, in Theorem 1, the uniqueness of solution for VO-ID-system (10) with the use of conditions in (H_1). In Theorem 2, the existence of solution for the VO-ID-system (10) is proved. Then HU-stability is derived in Theorem 3. In section 5, a computational algorithm is obtained with the help of LI polynomial. An illustrative example is given for the application of the presumed VO-ID-system (10) as a chaotic power system. Which is then studied in the fractional version for the control in the upcoming portions of the paper.

The discussion also focuses on the results obtained from the numerical simulation of the proposed adaptive fixed-time SMC method. The proposed control method and FFoSMC undergo a thorough examination simultaneously. Therefore, a thorough examination of Figure 2 and Figure 3 demonstrates that the suggested controller demonstrates exceptional tracking abilities and achieves rapid error convergence within a specified time frame. Additionally, the control inputs are depicted in Figure 4, which demonstrates that the suggested approach demonstrates considerable amounts of smoothness. These figures provided compelling evidence to support the statement that the suggested control approach demonstrates higher performance in comparison to other existing methods. Moreover, the picking of the parameters to be used for the suggested control approach should align with the previously defined requirements, which specify that the parameter k_i and $\mathcal{K}_i$ must be greater than zero, and the parameters p_1, q_1, and ϑ must all fall within the range $(0, 1)$, and p_2 and q_2 must be > 1. Avoiding these issues will prevent the closed-loop system from maintaining fixed-time stability. To attain fixed-time stability, it is necessary to carefully choose the suitable values for the parameter k_i and $\mathcal{K}_i$.

9. Conclusion

The significance of FDEs is paramount in the realm of mathematical modeling and simulations, particularly in addressing dynamic problems within the fields of science and engineering. Various forms of fractional order operators are being employed by researchers due to their convenience and precision. The expansion of integer order calculus to encompass fractional orders is responsible for this phenomenon. The utilization of variable order operators is a notable extension of fractional order calculus. This work presents the construction of a VO system for a set of FDEs where the order is itself a continuous function $\vartheta^*(x) : \mathbb{R} \to (0, 1]$. The study of the constructed VO-ID-system (10) was divided into two main portions. They are the theoretical and numerical aspects of the presumed problem. The theoretical aspect includes the existence of positive solutions, uniqueness results for the solutions, and HUS for the coupled system of VO-ID-system (10). In the numerical aspect of the paper, we have established an iterative scheme.

In order to control the fractional dynamics of a nonlinear power system, an adaptive fixed-time fractional-order SMC was introduced. The suggested fractional-order SMC demonstrates the ability to reach convergence in a fixed time and provides satisfactory tracking performance. The implementation of the designed adaptive scheme is essential in order to address the challenge of compensating for the unknown system dynamics. Results from a comparison between the proposed control scheme and the FFoSMC method demonstrate that the suggested method achieves good tracking performance, fast convergence, and fixed-time stability. Moreover, the examination of predefined-time SMC can be included in the domain of investigation of nonlinear systems.

Acknowledgements

The authors (Saim Ahmed, Hasib Khan, Jehad Alzabut, and Ahmad Taher Azar) would like to thank Prince Sultan University, Riyadh, Saudi Arabia for their support. This paper is derived from a research grant funded by the Research, Development, and Innovation Authority (RDIA) - Kingdom of Saudi Arabia, with grant number (13382-

psu-2023-PSNU-R-3-1-EI-). Special acknowledgments are given to Automated Systems & Computing Lab (ASCL), Prince Sultan University, Riyadh, Saudi Arabia. Jehad Alzabut is also thankful to the OSTIM Technical University for his support.

Conflict of interest

The authors declare no conflict of interest and have equal contributions.

Authors contribution

All authors contributed equally to this manuscript.

Author Statement

Hasib Khan: Conceptualization, Methodology, Writing- Original draft preparation, Software; Saim Ahmed: Conceptualization, Methodology, Software, Writing-Original draft preparation; Jehad Alzabut: Methodology, Software, Writing-Original draft preparation; Ahmad Taher Azar: Conceptualization, Methodology, Writing- Original draft preparation, Software, Supervision and J.F. Gómez Aguilar: Conceptualization, Methodology, Writing-Original draft preparation, Software, Supervision. All authors read and approved the final manuscript.

Competing interests

The authors declare that there is no conflict of interest regarding the publication of this paper.

Availability of data and materials:

All of the authors claim that all the data can be accessed in our manuscript in the numerical simulation section.

References

[1] L. Debnath. A brief historical introduction to fractional calculus. *International Journal of Mathematical Education in Science and Technology*, 35(4):487–501, 2004.

[2] J. Tenreiro Machado, V. Kiryakova, and F. Mainardi. Recent history of fractional calculus. *Communications in Nonlinear Science and Numerical Simulation*, 16(3):1140–1153, 2011.

[3] J. Tenreiro Machado, A. M. Galhano, and J. J. Trujillo. Science metrics on fractional calculus development since 1966. *Fractional Calculus and Applied Analysis*, 16(2):479–500, 2013.

[4] J. Tenreiro Machado, A. M. S. F. Galhano, and J. J. Trujillo. On development of fractional calculus during the last fifty years. *Scientometrics*, 98(1):577–582, 2014.

[5] H. H. Ammar, A. T. Azar, R. Shalaby, and M. I. Mahmoud. Metaheuristic optimization of fractional order incremental conductance (FO-INC) maximum power point tracking (MPPT). *Complexity*, 2019:1–13, 2019.

[6] P. Bedi, A. Kumar, T. Abdeljawad, Z. A. Khan, and A. Khan. Existence and approximate controllability of hilfer fractional evolution equations with almost sectorial operators. *Advances in Difference Equations*, 2020(1):1–5, 2020.

[7] A. Devi, A. Kumar, T. Abdeljawad, and A. Khan. Stability analysis of solutions and existence theory of fractional langevin equation. *Alexandria Engineering Journal*, 60(4):3641–3647, 2021.

[8] P. Bedi, A. Kumar, T. Abdeljawad, and A. Khan. Existence of mild solutions for impulsive neutral hilfer fractional evolution equations. *Advances in Difference Equations*, 2020(1):1–6, 2020.

[9] I. Podlubny. *Fractional Differential Equations*. Academic Press, New York, 1999.

[10] K. Deimling. *Nonlinear Functional Analysis*. Springer-Verlag, New York, 1985.

[11] A. Ouannas, A. T. Azar, T. Ziar, and A. G. Radwan. Generalized synchronization of different dimensional integer-order and fractional order chaotic systems. *Studies in Computational Intelligence*, 688:671–697, 2017.

[12] M. Soliman, A. T. Azar, M. A. Saleh, and H. H. Ammar. Path planning control for 3-omni fighting robot using pid and fuzzy logic controller. In *AMLTA 2019*, volume 921, pages 442–452. Springer, 2020.

[13] K. J. Ansari, Asma, F. Ilyas, K. Shah, A. Khan, and T. Abdeljawad. On new updated concept for delay differential equations with piecewise caputo fractional-order derivative. *Waves in Random and Complex Media*, pages 1–20, 2023.

[14] H. Sun, A. Chang, Y. Zhang, and W. Chen. A review on variable-order fractional differential equations. *Fractional Calculus and Applied Analysis*, 22(1):27–59, 2019.

[15] H. T. Pedro, M. H. Kobayashi, J. M. Pereira, and C. F. Coimbra. Variable order modeling of diffusive-convective effects on flow past a sphere. *Journal of Vibration and Control*, 14(9):1659–1672, 2008.

[16] H. G. Sun, W. Chen, H. Wei, and Y. Q. Chen. A comparative study of constant-order and variable-order fractional models. *The European Physical Journal Special Topics*, 193(1):185–192, 2011.

[17] H. Sun, W. Chen, and Y. Chen. Variable-order fractional differential operators in anomalous diffusion modeling. *Physica A*, 388(21):4586–4592, 2009.

[18] F. Wu, R. Gao, J. Liu, and C. Li. New fractional variable-order creep model with short memory. *Applied Mathematics and Computation*, 380:125278, 2020.

[19] N. Wan-Arfah, M. Muzaimi, N. N. Naing, and V. Subramaniyan. Prognostic factors of stroke patients in suburban malaysia. *Electronic Journal of General Medicine*, 20(6):em545, 2023.

[20] S. I. Mohammad, A. A. Al-Momani, A. Vasudevan, et al. Innovation through intelligence: Mapping ai with bibliometric methods. In *Digital Transformation 2025*, pages 187–198. Springer, 2025.

[21] C. B. Yong, R. Thinakaran, N. H. Ismail, and S. A. Awwad. Math role-play game using lehmer's rng algorithm. *IJACSA*, 15(12), 2024.

[22] H. Khan, W. F. Alfwzan, R. Latif, J. Alzabut, and R. Thinakaran. Ai-based deep learning of the water cycle system. *Fractal and Fractional*, 9(6):361, 2025.

[23] H. Khan, J. Alzabut, M. Tounsi, and D. K. Almutairi. Ai-based data analysis of contaminant transportation. *Fractal & Fractional*, 9(2), 2025.

[24] S. Jun, J. Wu, and Y. Cheng. Nonlinear dynamic characteristics of a power-turbine rotor system with branching structure. *International Journal of Non-linear Mechanics*, 2022.

[25] Z. Rafique, M. Haris, S. M. Khalid, S. M. Muyeen, and Innocent Kamwa. Bibliographic review on power system oscillations damping. *International Journal of Electrical Power & Energy Systems*, 2022.

[26] J. Yuxi, H. Wei, C. Shijie, K. Jurgen, and Z. Meng. Dynamic network characteristics of power-electronics-based power systems. *Scientific Reports*, 2020.

[27] C. Shun-Chang. Controlling chaos through period-doubling bifurcations in attitude dynamics for power systems. *Mathematical Problems in Engineering*, 2020.

[28] S. Samir and H. Ahmad. Control of instable chaotic small power system. *Journal of Power and Energy Engineering*, 2015.

[29] Z. Zhonghua. Chaos control of oscillator circuit based on adaptive backstepping method. *2014 Chinese Control and Decision Conference (CCDC)*, 2014.

[30] J. Ni, L. Liu, C. Liu, X. Hu, and S. Li. Fast fixed-time nonsingular terminal sliding mode control and its application to chaos suppression in power system. *IEEE Transactions on Circuits and Systems II: Express Briefs*, 64(2):151–155, 2016.

[31] A. Abdul-Basset, F. R. T. Al-Hussein, A. Ouannas, T. C. Sun, H. Jahanshahi, and A. A. Aly. Chaos suppressing in a three-buses power system using an adaptive synergetic control method. *Electronics*, 2021.

[32] H. D. Chiang, C. W. Liu, P. P. Varaiya, F. F. Wu, and M. G. Lauby. Chaos in a simple power system. *IEEE Transactions on Power Systems*, 8(4):1407–1417, 1993.

[33] J. B. Wang, C. X. Liu, Y. Wang, and G. C. Zheng. Fixed time integral sliding mode controller and its application to the suppression of chaotic oscillation in power system. *Chinese Physics B*, 27(7):070503, 2018.

[34] L. Lin, Q. Wang, B. He, Y. Chen, X. Peng, and R. Mei. Adaptive predefined-time synchronization of two different fractional-order chaotic systems with time-delay. *IEEE Access*, 9:31908–31920, 2021.

[35] S. Huang and J. Wang. Fixed-time fractional-order sliding mode control for nonlinear power systems. *Journal of Vibration and Control*, 26(17-18):1425–1434, 2020.

[36] Y. Lv, Y. Zhang, Q. Liu, S. Wang, and D. Shi. Sliding mode control of two-parameter fourth-order chaos model of power system. *IEEE Transactions on Circuits and Systems II: Express Briefs*, 69(12):4849–4853, 2021.

[37] Z. Anjum, H. Zhou, S. Ahmed, and Y. Guo. Fixed time sliding mode control for disturbed robotic manipulator. *Journal of Vibration and Control*, 2023.

[38] Z. Zhixiong, W. Xingyi, and L. Hak-Keung. Finite-time fuzzy sliding mode control for nonlinear descriptor systems. *IEEE/CAA Journal of Automatica Sinica*, 2021.

[39] S. Ahmed and A. T. Azar. Enhanced tracking control for n-dof robotic manipulators: A fixed-time terminal sliding mode approach with time delay estimation. *Results in Engineering*, 24:102904, 2024.

[40] S. Ahmed, A. T. Azar, and E. Walid. Adaptive predefined-time fractional terminal sliding mode control for robotic dynamic systems. *Journal of Mathematics and Computer Science*, 41:550–563, 2026.

[41] S. Ahmed and A. T. Azar. Adaptive pd sliding mode control for robot dynamics using predefined-time approach. *International Journal of Dynamics and Control*, 13(3):100, 2025.

[42] R. Lin, F. Liu, V. Anh, and I. Turner. Stability and convergence of explicit finite-difference for variable-order diffusion. *Applied Mathematics and Computation*, 212:435–445, 2009.

[43] S. Banach. Sur les operations dans les ensembles abstraits et leur application aux equations integrales. *Fundamenta Mathematicae*, 3:133–181, 1922.